https://doi.org/10.5194/amt-2024-142
Preprint. Discussion started: 26 August 2024

Atmospheric Measurement Techniques Discussions

Estimating hourly ground-level aerosols using GEMS aerosol optical depth: A machine learning approach

Sungmin O[1], Ji Won Yoon[2], and Seon Ki Park[3]

[1]Department of Climate and Energy Systems Engineering, Ewha Womans University, Seoul, Republic of Korea
[2]Center for Climate/Environment Change Prediction Research, Ewha Womans University, Seoul, Republic of Korea
[3]Severe Storm Research Center, Ewha Womans University, Seoul, Republic of Korea

Correspondence: Seon Ki Park (spark@ewha.ac.kr)

Abstract. The Geostationary Environment Monitoring Spectrometer (GEMS) is the world's first ultraviolet–visible instrument for air quality monitoring in geostationary orbit. Since its launch in 2020, GEMS has provided hourly daytime air quality information over Asia. However, to date, validation and applications of these data are lacking. Here we evaluate the effectiveness of the first 1.5-year GEMS aerosol optical depth (AOD) data in estimating ground-level particulate matter (PM) concentrations at an hourly scale. To do so, we employ random forest models and use GEMS AOD data and meteorological variables as input features to estimate PM10 and PM2.5 concentrations, respectively, in South Korea. The model-estimated PM concentrations are strongly correlated with ground measurements, but they exhibit negative biases, particularly during high aerosol loading months. Our results indicate that GEMS AOD values represent underestimates compared to ground-measured AOD values, possibly leading to negative biases in the final PM estimates. Further, we demonstrate that more training data could significantly improve random forest model performance, thus indicating the potential of GEMS for high-resolution surface PM prediction when sufficient data are accumulated over the coming years. Our results will serve as a reference to aid the evaluation of future GEMS AOD retrieval algorithm improvements and also provide initial guidance for data users.

1 Introduction

The adverse impacts of particulate matter (PM) on human health are well known. Exposure to high PM concentration can cause serious health risks such as cancers, respiratory and cardiovascular diseases (Chen and Hoek, 2020; Kim and Kim, 2020; Ciabattini et al., 2021; Moreno-Ríos et al., 2022). PM can also have a harmful effect on ecosystems through deposition of PM and its subsequent uptake by plants (Rai, 2016; Roy et al., 2024). Accordingly, in many countries, it is mandatory to control ambient PM concentrations, and regular PM concentration measurements are key to designing appropriate policies to constrain the presence of PM. Given this background, the number of air quality monitoring stations has been growing worldwide; however, these ground-based measurement stations are often concentrated in city areas only and insufficiently densely distributed

https://doi.org/10.5194/amt-2024-142
Preprint. Discussion started: 26 August 2024

to provide spatially continuous data (Martin et al., 2019).

In contrast, satellite observational data, with its broad spatial coverage, can be potentially used to improve air quality monitoring (including PM) on a regional to global scale. In this context, the Geostationary Environmental Monitoring Spectrometer (GEMS) onboard the Geostationary Korea Multi-Purpose Satellite-2B (GEO-KOMPSAT-2B), which was launched in 2020 by the Republic of Korea, aims for near real-time monitoring of air quality over Asia (Kim et al., 2020) where air quality is the one of biggest environmental health risks (Hopke et al., 2008). As the first ultraviolet (UV)–visible instrument in a geosynchronous orbit, GEMS can provide more detailed and frequent air quality data than existing low Earth orbit platforms. Since the first release of the GEMS data, some verification of its initial air pollutant products including nitrogen dioxide or ozone has recently been performed (e.g. Baek et al., 2023; Kim et al., 2023; Ghahremanloo et al., 2024). However, data validation and applications of many GEMS products are still largely lacking.

We focus on the GEMS aerosol optical depth (AOD), which measures the degree of light scattering or absorption at a given wavelength due to the presence of aerosols in the atmospheric column (Chudnovsky et al., 2012). Satellite-derived AOD has been widely used to predict ground-level PM concentrations (Shin et al., 2020), as can be seen in the example of Moderate Resolution Imaging Spectroradiometer or Geostationary Operational Environmental Satellite (Chudnovsky et al., 2012; Gupta et al., 2006; Yang et al., 2020; Zhai et al., 2021; Hammer et al., 2023). Nonetheless, inconsistent relationships between satellite-derived AOD and ground-level PM observations have been reported among different regions and based on data from different satellite instruments (Yang et al., 2020). Therefore, there is an urgent need to evaluate the effectiveness of GEMS AOD data in estimating PM concentrations over Asia, which can in turn provide initial guidance for both data users and algorithm developers.

In this study, we use GEMS AOD data over South Korea during the first 1.5 years of observations from January 2022 through to June 2023 (the very first data are available from November 2021). In Korea, publicly available PM measurement data (PM10 and PM2.5), which can serve as continuous ground reference, can be obtained from nationwide air quality monitoring stations. To convert the AOD from satellite observations into surface PM concentrations, we employ the random forest (RF), which is a very popular machine learning method for PM estimation given its great flexibility and strong predictive performance (Shin et al., 2020; Hu et al., 2017; Guo et al., 2021). At each station, we train an RF model using GEMS AOD data and relevant meteorological variables as input features and predict the PM concentrations at an hourly scale using the trained models. We then evaluate the RF model performance and examine biases observed in the estimated PM concentrations. Consequently, our study aims to demonstrate the usefulness of GEMS AOD in PM modelling and limitations in the current version of the data.

https://doi.org/10.5194/amt-2024-142
Preprint. Discussion started: 26 August 2024

Atmospheric Measurement Techniques Discussions

2 Data and methods

The hourly PM concentration data in South Korea for the period of January 2022 to June 2023 used in this study are obtained from the AirKorea real-time ambient air quality monitoring system (https://www.airkorea.or.kr/) operated by the Korea Environment Corporation. The PM concentrations are determined using a β-ray absorption method, and the measurements have undergone quality controls to remove anomalous values before the release of the final data.

GEMS on board the GEO-COMPSAT-2B satellite has been in operation since 2020. The GEMS instrument measures the UV-visible radiance spectrum, and its geostationary orbit allows AOD retrievals to be obtained at an hourly frequency during cloud-free daytime conditions (Kim et al., 2020). The GEMS aerosol products provide AOD at three wavelength channels with a nominal spatial resolution of 3.5 km x 8 km at Seoul. Details about the GEMS aerosol retrievals can be found from GEMS ATBD ARA (2020). We use GEMS AOD Level 2 (L2) data (at 443 nm) within a $\pm$ 15 min time window of the PM10 measurement times, extracted at the pixel nearest to the AirKorea monitoring stations (within a distance of 2.02 km on average).

The relationship between AOD and PM concentrations can be affected by meteorological conditions (Koelemeijer et al., 2006; Tian and Chen, 2010; Handschuh et al., 2022). We consider boundary layer height (BLH), relative humidity (RH), air temperature (TEMP), surface pressure (SP), and wind speed and direction (WS and WD, respectively) as input features, in addition to AOD, to estimate the PM concentrations using RF models. BLH data from ERA5 reanalysis at a 0.25-degree resolution are employed as a proxy for the vertical aerosol concentration in the lower troposphere as AOD is assumed to represent attenuation in the boundary layer (Gupta and Christopher, 2009b). The other variables are all obtained from ERA5-Land at a 0.1-degree resolution. RH is computed using temperature and dew temperature (Lawrence, 2005), while wind speed and direction are calculated using u and v wind components. Both ERA5 and ERA5-Land data are available at an hourly temporal resolution (Hersbach et al., 2020), and we thus select the data at the closest PM ground measurement times and locations.

For the AOD-PM simulations, we employ an RF algorithm with 100 trees and train this algorithm using AOD and meteorological data as input features and ground PM measurements as the target variable, respectively. To evaluate the model performance, we randomly split the entire data into five subgroups and use four of them (80%) as training data and the remainder (20%) as validation data. This process is repeated five times such that every data subset is used as validation data at least once (i.e. five-fold cross-validation).

2.1 Results and Discussion

Air quality, including PM concentrations, is routinely monitored in Korea via the AirKorea air quality monitoring network. Out of more than 600 ground-based AirKorea stations, we select a total of 456 urban air quality monitoring stations to represent human exposure to PM (Fig. 1). While the stations are distributed across the country, a large number of stations are concen-

https://doi.org/10.5194/amt-2024-142
Preprint. Discussion started: 26 August 2024

trated in the densely populated Seoul Capital Area, located in the northwest of the study domain. We obtain the GEMS AOD values that match the locations and measurements times of the ground PM data as closely as possible (see Methods), resulting in an average of 1496 data pairs at each station. Note that GEMS provides hourly observations of AOD during the daytime, corresponding to six to ten times per day depending on the season.

Figure 1a shows the average PM10 concentrations at the selected stations during the study period, calculated only when AOD observation data are available (i.e. collocated PM and AOD data pairs). The average PM10 across the stations is 41.43 $\mu g\ m^{-3}$, ranging from 25.80 to 65.10 $\mu g\ m^{-3}$, which is higher than actual PM10 averages during the same period when night-time data are also included (Fig. S1 in Supplementary). Overall, relatively high PM10 concentrations are observed in western regions, which are related to strong inflow from the continent due to the prevailing mid-latitude westerlies in South Korea (Lee et al., 2019).

Next, we estimate ground-level PM10 concentrations using RF models, which are trained individually at each station using AOD values and meteorological variables as input features (See Methods). RF can effectively handle non-linear relationships between input features and target variables, making it a useful tool for air quality modelling applications. We also confirm that RF outperforms linear regression models in estimating PM10 (Fig. S2); all model performances are evaluated through the five-fold cross validation.

Overall, the RF models demonstrate satisfactory PM10 estimation performance. The spatial distribution of PM10 concentrations observed in the measurements is effectively described by the model estimates (Fig. 1b), with an average estimated PM10 value of 41.66 $\mu g\ m^{-3}$, ranging from 25.92 to 65.61 $\mu g\ m^{-3}$, which closely matches the average measured value. The Pearson's correlation coefficients (r-value) between the measured and estimated PM10 is 0.65, on average, across all the stations (Fig. 1c). The model performance is stable across the stations, as indicated by the correlation values between 0.59 to 0.70 (10th and 90th percentiles, respectively) at most stations. We also obtain similar PM2.5 estimation results using the RF models (see Fig. S3).

The entire data combined from all stations are also compared. As shown in Fig. 2a, the AOD and PM10 show a positive, but weak correlation with an r-value of 0.25, thus indicating that the relationship between columnar AOD and ground-level PM10 is non-trivial. Meanwhile, AOD-estimated PM10 values are in better agreement with the ground measurements (r-value of 0.67), but exhibit significant negative biases (Fig. 2b), which will be further investigated in the following section. The RF models also show similar performance in the case of PM2.5 (Fig. S4).

Furthermore, we use SHapley Additive exPlanations (SHAP) to quantify the relative importance of the considered input features on the model's predictions. SHAP is an explainable machine learning method based on Shapley values, which measure the marginal contribution of each predictor to the model's output or prediction across all the possible predictor combinations

https://doi.org/10.5194/amt-2024-142
Preprint. Discussion started: 26 August 2024

(Lundberg et al., 2020; Molnar, 2019). We take the mean of absolute SHAP values for each input variable across all the predictions to explain its global feature contributions (Fig. 3).

While AOD has the greatest influence on the model performance, as expected from its relatively strong correlation with ground aerosols (Fig. 2a and Fig. S5), the temperature and boundary layer height (TEMP and BLH, respectively) appear as the most influential predictors among the considered meteorological variables. The TEMP and BLH show relatively strong correlations with PM10 (Fig. S5), and their contributions to the prediction confirm the usefulness of RF models in capturing complex, nonlinear input-output relationships. For instance, temperature can promote PM particle production by enhancing the photochemical reactions in the atmosphere (Gupta and Christopher, 2009a). It can also act as an indicator of seasonal variations in PM concentrations; for instance, an increase in emissions from combustion processes during the winter time can result in high aerosol loading, while aerosols can easily be removed by wet deposition during a rainy season in summer (Kim and Kim, 2020). Given that aerosols are primarily confined to the planetary boundary layer, BLH is a good proxy with which estimate the height of the aerosol layer (Lee et al., 2024) and can help relate columnar satellite data to surface aerosol values (Handschuh et al., 2022; Gupta and Christopher, 2009a).

We further compare the temporal evolution of hourly PM10 measurements and estimates in each month. The PM10 observations in Fig. 4a displays clear seasonal patterns, with high concentrations recorded during the winter and spring months and low concentrations in the autumn. While PM10 values in South Korea often show strong diurnal or semidiurnal cycles (Kim and Kim, 2020), these diurnal variations are not clearly shown in these PM10 composites from multiple stations, which contain many gaps due to the missing values in the satellite data. The high concentrations during the cold season (winter to early spring) can be attribute to increased fossil fuel combustion for heating combined with the stagnant weather conditions during this season (Wang et al., 2015). Particularly in March, the highest PM10 is associated with the long-range transport of Asian dust originating in the deserts of Mongolia and China (Lee et al., 2019, 2024; Kim et al., 2017). These seasonal variations are also well captured in the estimated PM10 concentrations (Fig. 4b), and the overall pattern is in good agreement with that of the ground measurements. The spatial correlation between the measured and estimated PM10 concentrations (Fig. 4a and Fig. 4b, respectively) is 0.95. Yet, we observe substantial differences in the magnitude, as shown in Fig. 4c, with underestimation of high values during the winter and spring and overestimation of low values in the autumn. We also observe similar contrasting biases between the seasons, but with smaller magnitudes for the PM2.5 (Fig. S6).

The underestimation of very high values, such as those observed in March, by machine learning methods is unsurprising given that these rare values are not well-represented in the training data. Nonetheless, as AOD is found to be the most influential input feature for the predictive ability of the RF models (Fig. 3), we assume that the quality of the AOD can directly affect the models' performance. To confirm this, we further compare the GEMS AOD data with ground-based AOD measurements from the AErosol RObotic NETwork (AERONET) (Giles et al., 2019). We use AERONET Version 3 Level 2.0 quality-assured data from the six sites in South Korea (see Fig. S7 for the location of the sites). Note that as we extract the closest GEMS AOD data point to each AERONET site, the GEMS data used in this additional analysis are not directly comparable with those used in the previous analysis. Nevertheless, we find that the GEMS tends to underestimate AOD, compared to the ground-based AOD measurements (Fig. 5). A study on the early version of GEMS L2 algorithm prior to the launch of GEMS also reported high correlation, but slight underestimation of GEMS AOD compared to AERONET (Kim et al., 2020).

Overall, negative biases are prevalent during the spring, particularly in March and April, while weak positive biases are observed during the autumn and early winter (September to December). These trends are broadly consistent with the bias patterns identified in the PM10 estimates (see Fig. 4). AOD retrievals from satellite observations can be influenced by many factors, including surface reflectance estimation or aerosol model assumptions. For instance, neglecting the nonsphericity of dust in the satellite algorithm usually leads to underestimation of AOD retrievals under dusty conditions (Feng et al., 2009). In addition, distinguishing surface reflectance and aerosol scattering or absorption effect can be challenging under low aerosol loading conditions (Rudke et al., 2023). Other issues such as cloud contamination or heterogeneous surface conditions also can lead to uncertainties in satellite-derived AOD (Handschuh et al., 2022). Consequently, data uncertainties in GEMS AOD likely affect the performance of RF, given that input data quality has a significant impact on the trained machine learning model's predictions.

Finally, we examine the potential of improving RF performance using larger training data. GEMS has started its data observation in early 2020 and, moreover, it has significant data gaps, for instance, in cloudy conditions. Thus, there are currently insufficient data for a broad range of applications. The performance of machine learning is highly dependent not only on the training data quality but also on the quantity and diversity of the data (O et al., 2020). In this context, we retrain an RF model at each station with a larger training data volume by utilising data from its n neighbouring stations. The model validation is performed five times using a random 20% split of each station's training data each time, per the approach used in the main analysis.

Fig. 6 demonstrates that the RF models' performance can be improved by including more training data. Compared to the model performance without additional training data from neighbouring stations ($n = 0$), the RF models with data supplement show higher correlation coefficients and decreased negative biases. Comparing the original model and the model constructed with data from eight neighbouring stations, the site-averaged r-value increases from 0.7 to 0.8 and the regression slope increases from 0.4 to 0.7.

3 Conclusions

Applying satellite-derived AOD observational data to estimate ground-level PM offers an excellent opportunity for air quality monitoring, including at ungauged sites (Hammer et al., 2023; Filonchyk et al., 2020; Wei et al., 2023). This is particularly important for Asian regions, where a significant proportion of the population is exposed to air pollution levels exceeding WHO

https://doi.org/10.5194/amt-2024-142
Preprint. Discussion started: 26 August 2024

guideline values (Cohen et al., 2017). As the world's first geostationary earth orbit environmental instrument, GEMS is expected to provide more detailed air quality information over Asia with higher spatial and temporal resolutions than existing low Earth orbit platforms. GEMS will also join a constellation of geostationary air quality satellites, together with TEMPO over North America and Sentinel-4 over Europe, to collectively provide near-global coverage (Kim et al., 2020). In line with ongoing efforts to confirm the reliability of the new satellite data products, in this study, we evaluate the effectiveness of GEMS AOD data by modelling AOD-PM relationships at over 400 stations in South Korea using RF models.

While using the GEMS AOD data alone yields limited predictive performance, including meteorological variables such as temperature and boundary layer height allows the model-estimated PM concentrations to reach strong correlations (r-values > 0.65) with ground measurements both temporally and spatially. Nonetheless, underestimation biases in the GEMS AOD compared to the ground-measured AOD, especially during high-PM months, could lead to negative biases in the final PM estimation. Such data uncertainties should be carefully considered in future satellite retrieval algorithms and data applications.

Given that only the first 1.5-year GEMS data are used in this study, we also demonstrate that larger training data volumes can potentially improve the performance of PM estimation, implying that the availability of longer data archives in the near future will allow estimation models to be further refined. More sophisticated machine learning algorithms or different modelling approaches (e.g. chemical transport models) could also lead to improved PM predictions from satellite AOD, and our findings in this study can serve as a baseline for comparison of different methods in future studies. Moreover, after accumulating a larger volume of GEMS data, the AOD data should be evaluated from more diverse perspectives, including diurnal variations at a certain location or PM estimation at ungauged locations.

Code availability. Code supporting this paper is published online at https://github.com/osungmin/gems_aod.

Data availability. GEMS AOD data can be requested from the Environmental Satellite Center website (https://nesc.nier.go.kr/). PM measurement data is publicly available from the AirKorea website (https://www.airkorea.or.kr/). ERA5 and ERA5-Land can be freely downloaded from the Climate Data Store of the Copernicus Climate Change Service (https://cds.climate.copernicus.eu/).

Author contributions. SO designed the study, performed the experiments, and drafted the manuscript. JWY and SKP discussed the results and contributed to the writing.

Competing interests. The authors declare that they have no conflict of interest.

https://doi.org/10.5194/amt-2024-142
Preprint. Discussion started: 26 August 2024

Acknowledgements. This work is supported by the National Research Foundation of Korea (NRF) grant funded by the Korea government (MSIT) (2021R1A2C1095535) and partly by Basic Science Research Program through the NRF funded by the Ministry of Education (2018R1A6A1A08025520). SKP is partly supported by the Specialized university program for confluence analysis of Weather and Climate Data of the Korea Meteorological Institute (KMI) funded by the Korean government (KMA). SO acknowledges the Basic Science Research Program through the National Research Foundation of Korea (NRF) funded by the Ministry of Education (RS-2023-00248706). The authors thank the principal investigators of each AERONET site for their efforts in establishing and maintaining the AERONET sites (https://aeronet.gsfc.nasa.gov/) the data of which are used in the study.

https://doi.org/10.5194/amt-2024-142
Preprint. Discussion started: 26 August 2024

References

Baek, K., Kim, J. H., Bak, J., Haffner, D. P., Kang, M., and Hong, H.: Evaluation of total ozone measurements from Geostationary Environmental Monitoring Spectrometer (GEMS), Atmos. Meas. Tech., 16, 5461–5478, https://doi.org/10.5194/amt-16-5461-2023, 2023.

Chen, J. and Hoek, G.: Long-term exposure to PM and all-cause and cause-specific mortality: A systematic review and meta-analysis, Environ. Int., 143, 105 974, https://doi.org/10.1016/j.envint.2020.105974, 2020.

Chudnovsky, A. A., Lee, H. J., Kostinski, A., Kotlov, T., and Koutrakis, P.: Prediction of daily fine particulate matter concentrations using aerosol optical depth retrievals from the Geostationary Operational Environmental Satellite (GOES), J. Air Waste Manag. Assoc., 62, 1022–1031, https://doi.org/10.1080/10962247.2012.695321, 2012.

Ciabattini, M., Rizzello, E., Lucaroni, F., Palombi, L., and Boffetta, P.: Systematic review and meta-analysis of recent high-quality studies on exposure to particulate matter and risk of lung cancer, Environ. Res., 196, 110 440, https://doi.org/10.1016/j.envres.2020.110440, 2021.

Cohen, A. J., Brauer, M., Burnett, R., Anderson, H. R., Frostad, J., Estep, K., Balakrishnan, K., Brunekreef, B., Dandona, L., Dandona, R., Feigin, V., Freedman, G., Hubbell, B., Jobling, A., Kan, H., Knibbs, L., Liu, Y., Martin, R., Morawska, L., Pope, C. A., Shin, H., Straif, K., Shaddick, G., Thomas, M., Van Dingenen, R., Van Donkelaar, A., Vos, T., Murray, C. J. L., and Forouzanfar, M. H.: Estimates and 25-year trends of the global burden of disease attributable to ambient air pollution: an analysis of data from the Global Burden of Diseases Study 2015, Lancet, 389, 1907–1918, https://doi.org/10.1016/S0140-6736(17)30505-6, 2017.

Feng, Q., Yang, P., Kattawar, G. W., Hsu, C. N., Tsay, S.-C., and Laszlo, I.: Effects of particle nonsphericity and radiation polarization on retrieving dust properties from MODIS observations, J. Aerosol Sci., 40, 776–789, https://doi.org/10.1016/j.jaerosci.2009.05.001, 2009.

Filonchyk, M., Hurynovich, V., and Yan, H.: Trends in aerosol optical properties over Eastern Europe based on MODIS-Aqua, Geosci. Front., 11, 2169–2181, https://doi.org/10.1016/j.gsf.2020.03.014, 2020.

Ghahremanloo, M., Choi, Y., and Singh, D.: Deep learning bias correction of GEMS tropospheric NO2: A comparative validation of NO2 from GEMS and TROPOMI using Pandora observations, Environ Int, 190, 108 818, https://doi.org/10.1016/j.envint.2024.108818, 2024.

Giles, D. M., Sinyuk, A., Sorokin, M. G., Schafer, J. S., Smirnov, A., Slutsker, I., Eck, T. F., Holben, B. N., Lewis, J. R., Campbell, J. R., Welton, E. J., Korkin, S. V., and Lyapustin, A. I.: Advancements in the Aerosol Robotic Network (AERONET) Version 3 database – automated near-real-time quality control algorithm with improved cloud screening for Sun photometer aerosol optical depth (AOD) measurements, Atmos. Meas. Tech., 12, 169–209, https://doi.org/10.5194/amt-12-169-2019, 2019.

Guo, B., Zhang, D., Pei, L., Su, Y., Wang, X., Bian, Y., Zhang, D., Yao, W., Zhou, Z., and Guo, L.: Estimating PM2.5 concentrations via random forest method using satellite, auxiliary, and ground-level station dataset at multiple temporal scales across China in 2017, Sci. Total Environ., 778, 146 288, https://doi.org/10.1016/j.scitotenv.2021.146288, 2021.

Gupta, P. and Christopher, S. A.: Particulate matter air quality assessment using integrated surface, satellite, and meteorological products: 2. A neural network approach, J. Geophys. Res., 114, 2008JD011 497, https://doi.org/10.1029/2008JD011497, 2009a.

Gupta, P. and Christopher, S. A.: Particulate matter air quality assessment using integrated surface, satellite, and meteorological products: Multiple regression approach, J. Geophys. Res., 114, 2008JD011 496, https://doi.org/10.1029/2008JD011496, 2009b.

Gupta, P., Christopher, S. A., Wang, J., Gehrig, R., Lee, Y., and Kumar, N.: Satellite remote sensing of particulate matter and air quality assessment over global cities, Atmos. Environ., 40, 5880–5892, https://doi.org/10.1016/j.atmosenv.2006.03.016, 2006.

Hammer, M. S., Van Donkelaar, A., Bindle, L., Sayer, A. M., Lee, J., Hsu, N. C., Levy, R. C., Sawyer, V., Garay, M. J., Kalashnikova, O. V., Kahn, R. A., Lyapustin, A., and Martin, R. V.: Assessment of the impact of discontinuity in satellite instruments and retrievals on global PM2.5 estimates, Remote Sens. Environ., 294, 113 624, https://doi.org/10.1016/j.rse.2023.113624, 2023.

Handschuh, J., Erbertseder, T., Schaap, M., and Baier, F.: Estimating PM2.5 surface concentrations from AOD: A combination of SLSTR and MODIS, Remote Sens. Appl.: Soc. Environ., 26, https://doi.org/10.1016/j.rsase.2022.100716, 2022.

Hersbach, H., Bell, B., Berrisford, P., Hirahara, S., Horányi, A., Muñoz-Sabater, J., Nicolas, J., Peubey, C., Radu, R., Schepers, D., Simmons, A., Soci, C., Abdalla, S., Abellan, X., Balsamo, G., Bechtold, P., Biavati, G., Bidlot, J., Bonavita, M., De Chiara, G., Dahlgren, P., Dee, D., Diamantakis, M., Dragani, R., Flemming, J., Forbes, R., Fuentes, M., Geer, A., Haimberger, L., Healy, S., Hogan, R. J., Hólm, E., Janisková, M., Keeley, S., Laloyaux, P., Lopez, P., Lupu, C., Radnoti, G., De Rosnay, P., Rozum, I., Vamborg, F., Villaume, S., and Thépaut, J.: The ERA5 global reanalysis, Quart J Royal Meteoro Soc, 146, 1999–2049, 2020.

Hopke, P. K., Cohen, D. D., Begum, B. A., Biswas, S. K., Ni, B., Pandit, G. G., Santoso, M., Chung, Y.-S., Davy, P., Markwitz, A., Waheed, S., Siddique, N., Santos, F. L., Pabroa, P. C. B., Seneviratne, M. C. S., Wimolwattanapun, W., Bunprapob, S., Vuong, T. B., Duy Hien, P., and Markowicz, A.: Urban air quality in the Asian region, Sci. Total Environ., 404, 103–112, https://doi.org/10.1016/j.scitotenv.2008.05.039, 2008.

Hu, X., Belle, J. H., Meng, X., Wildani, A., Waller, L. A., Strickland, M. J., and Liu, Y.: Estimating $PM_{2.5}$ concentrations in the conterminous United States using the random forest approach, Environ. Sci. Technol., 51, 6936–6944, https://doi.org/10.1021/acs.est.7b01210, 2017.

Kim, H. C., Kim, E., Bae, C., Cho, J. H., Kim, B.-U., and Kim, S.: Regional contributions to particulate matter concentration in the Seoul metropolitan area, South Korea: seasonal variation and sensitivity to meteorology and emissions inventory, Atmos. Chem. Phys., 17, 10 315–10 332, https://doi.org/10.5194/acp-17-10315-2017, 2017.

Kim, J., Jeong, U., Ahn, M.-H., Kim, J. H., Park, R. J., Lee, H., Song, C. H., Choi, Y.-S., Lee, K.-H., Yoo, J.-M., Jeong, M.-J., Park, S. K., Lee, K.-M., Song, C.-K., Kim, S.-W., Kim, Y. J., Kim, S.-W., Kim, M., Go, S., Liu, X., Chance, K., Chan Miller, C., Al-Saadi, J., Veihelmann, B., Bhartia, P. K., Torres, O., Abad, G. G., Haffner, D. P., Ko, D. H., Lee, S. H., Woo, J.-H., Chong, H., Park, S. S., Nicks, D., Choi, W. J., Moon, K.-J., Cho, A., Yoon, J., Kim, S.-k., Hong, H., Lee, K., Lee, H., Lee, S., Choi, M., Veefkind, P., Levelt, P. F., Edwards, D. P., Kang, M., Eo, M., Bak, J., Baek, K., Kwon, H.-A., Yang, J., Park, J., Han, K. M., Kim, B.-R., Shin, H.-W., Choi, H., Lee, E., Chong, J., Cha, Y., Koo, J.-H., Irie, H., Hayashida, S., Kasai, Y., Kanaya, Y., Liu, C., Lin, J., Crawford, J. H., Carmichael, G. R., Newchurch, M. J., Lefer, B. L., Herman, J. R., Swap, R. J., Lau, A. K. H., Kurosu, T. P., Jaross, G., Ahlers, B., Dobber, M., McElroy, C. T., and Choi, Y.: New era of air quality monitoring from space: Geostationary Environment Monitoring Spectrometer (GEMS), Bull. Am. Meterol. Soc., 101, E1–E22, https://doi.org/10.1175/BAMS-D-18-0013.1, 2020.

Kim, S., Kim, D., Hong, H., Chang, L.-S., Lee, H., Kim, D.-R., Kim, D., Yu, J.-A., Lee, D., Jeong, U., Song, C.-K., Kim, S.-W., Park, S. S., Kim, J., Hanisco, T. F., Park, J., Choi, W., and Lee, K.: First-time comparison between NO_2 vertical columns from Geostationary Environmental Monitoring Spectrometer (GEMS) and Pandora measurements, Atmos. Meas. Tech., 16, 3959–3972, https://doi.org/10.5194/amt-16-3959-2023, 2023.

Kim, S.-U. and Kim, K.-Y.: Physical and chemical mechanisms of the daily-to-seasonal variation of PM10 in Korea, Sci. Total Environ., 712, 136 429, https://doi.org/10.1016/j.scitotenv.2019.136429, 2020.

Koelemeijer, R., Homan, C., and Matthijsen, J.: Comparison of spatial and temporal variations of aerosol optical thickness and particulate matter over Europe, Atmos. Environ., 40, 5304–5315, https://doi.org/10.1016/j.atmosenv.2006.04.044, 2006.

Lawrence, M. G.: The relationship between relative humidity and the dewpoint temperature in moist air: a simple conversion and applications, Bull. Amer. Meteor. Soc., 86, 225–234, https://doi.org/10.1175/BAMS-86-2-225, 2005.

Lee, H.-J., Jo, H.-Y., Kim, S.-W., Park, M.-S., and Kim, C.-H.: Impacts of atmospheric vertical structures on transboundary aerosol transport from China to South Korea, Sci Rep, 9, 13 040, https://doi.org/10.1038/s41598-019-49691-z, 2019.

Lee, S., Yoon, J., and Park, S. K.: Primary factors and synoptic pattern classification of mega Asian dust storms in Korea, Asia-Pac. J. Atmos. Sci., https://doi.org/in print, 2024.

Lundberg, S. M., Erion, G., Chen, H., DeGrave, A., Prutkin, J. M., Nair, B., Katz, R., Himmelfarb, J., Bansal, N., and Lee, S.-I.: From local explanations to global understanding with explainable AI for trees, Nat Mach Intell, 2, 56–67, https://doi.org/10.1038/s42256-019-0138-9, 2020.

Martin, R. V., Brauer, M., Van Donkelaar, A., Shaddick, G., Narain, U., and Dey, S.: No one knows which city has the highest concentration of fine particulate matter, Atmos. Environ.: X, 3, 100 040, https://doi.org/10.1016/j.aeaoa.2019.100040, 2019.

Molnar, C.: Interpretable Machine Learning, https://christophm.github.io/interpretable-ml-book/, 2019.

Moreno-Ríos, A. L., Tejeda-Benítez, L. P., and Bustillo-Lecompte, C. F.: Sources, characteristics, toxicity, and control of ultrafine particles: An overview, Geosci. Front, 13, 101 147, https://doi.org/10.1016/j.gsf.2021.101147, 2022.

O, S., Dutra, E., and Orth, R.: Robustness of process-based versus data-driven modeling in changing climatic conditions, J. Hydrometeorol., 21, 1929–1944, https://doi.org/10.1175/JHM-D-20-0072.1, 2020.

Rai, P. K.: Impacts of particulate matter pollution on plants: Implications for environmental biomonitoring, Ecotoxicol Environ Saf, 129, 120–136, https://doi.org/10.1016/j.ecoenv.2016.03.012, 2016.

Roy, A., Mandal, M., Das, S., Popek, R., Rakwal, R., Agrawal, G. K., Awasthi, A., and Sarkar, A.: The cellular consequences of particulate matter pollutants in plants: Safeguarding the harmonious integration of structure and function, Sci. Total Environ., 914, 169 763, https://doi.org/10.1016/j.scitotenv.2023.169763, 2024.

Rudke, A. P., Martins, J. A., Martins, L. D., Vieira, C. L. Z., Li, L., Assunção Da Silva, C. F., Dos Santos, A. M., Koutrakis, P., and De Almeida Albuquerque, T. T.: Evaluation and comparison of MODIS aerosol optical depth retrieval algorithms over Brazil, Atmos. Environ., 314, 120 130, https://doi.org/10.1016/j.atmosenv.2023.120130, 2023.

Shin, M., Kang, Y., Park, S., Im, J., Yoo, C., and Quackenbush, L. J.: Estimating ground-level particulate matter concentrations using satellite-based data: a review, GISci. Remote Sens., 57, 174–189, https://doi.org/10.1080/15481603.2019.1703288, 2020.

Tian, J. and Chen, D.: A semi-empirical model for predicting hourly ground-level fine particulate matter (PM2.5) concentration in southern Ontario from satellite remote sensing and ground-based meteorological measurements, Remote Sens. Environ., 114, 221–229, https://doi.org/10.1016/j.rse.2009.09.011, 2010.

Wang, Y. Q., Zhang, X. Y., Sun, J. Y., Zhang, X. C., Che, H. Z., and Li, Y.: Spatial and temporal variations of the concentrations of PM10, PM2.5 and PM1 in China, Atmos. Chem. Phys., 15, 13 585–13 598, https://doi.org/10.5194/acp-15-13585-2015, 2015.

Wei, J., Li, Z., Lyapustin, A., Wang, J., Dubovik, O., Schwartz, J., Sun, L., Li, C., Liu, S., and Zhu, T.: First close insight into global daily gapless 1 km PM2.5 pollution, variability, and health impact, Nat Commun, 14, 8349, https://doi.org/10.1038/s41467-023-43862-3, 2023.

Yang, Z., Zdanski, C., Farkas, D., Bang, J., and Harris Williams: Evaluation of Aerosol Optical Depth (AOD) and PM2.5 associations for air quality assessment, Remote Sens. Appl.: Soc. Environ., 20, 100 396, https://doi.org/10.1016/j.rsase.2020.100396, 2020.

Zhai, S., Jacob, D. J., Brewer, J. F., Li, K., Moch, J. M., Kim, J., Lee, S., Lim, H., Lee, H. C., Kuk, S. K., Park, R. J., Jeong, J. I., Wang, X., Liu, P., Luo, G., Yu, F., Meng, J., Martin, R. V., Travis, K. R., Hair, J. W., Anderson, B. E., Dibb, J. E., Jimenez, J. L., Campuzano-Jost, P., Nault, B. A., Woo, J.-H., Kim, Y., Zhang, Q., and Liao, H.: Relating geostationary satellite measurements of aerosol optical depth (AOD) over East Asia to fine particulate matter (PM): insights from the KORUS-AQ aircraft campaign and GEOS-Chem model simulations, Atmos. Chem. Phys., 21, 16 775–16 791, https://doi.org/10.5194/acp-21-16775-2021, 2021.

https://doi.org/10.5194/amt-2024-142
Preprint. Discussion started: 26 August 2024

Atmospheric Measurement Techniques
Discussions

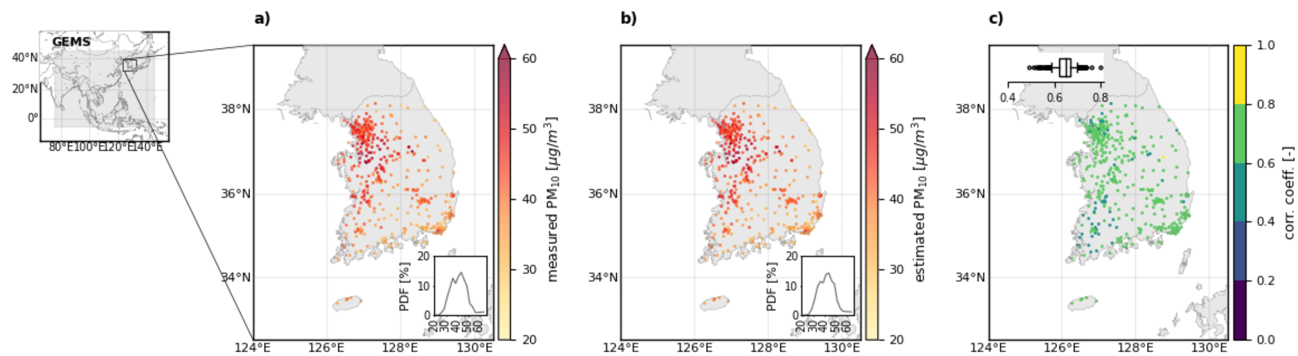

Figure 1. Comparison of measured and model-estimated PM10 concentrations over South Korea. Grey area in the small map (the leftmost panel) shows the spatial coverage of GEMS (5°S–45°N, 75°E–145°E) over Asia, including South Korea marked by a black box, which is enlarged for detailed analyses at urban air quality monitoring stations for the period of January 2022 to June 2023. Average of (a) the measured and (b) estimated PM10 concentrations, and (c) correlations of the measured and estimated PM10 values at each station. Note that only the data pairs which both PM and GEMS AOD data are available are included. The inset plots in (a) and (b) show the probability density function (PDF) of PM10. In the inset plot of (c), the box represents the interquartile range, where the vertical centre line is the median, and the whiskers represent the 10th and 90th percentiles, with outliers shown as dots.

Atmospheric Measurement Techniques
Discussions

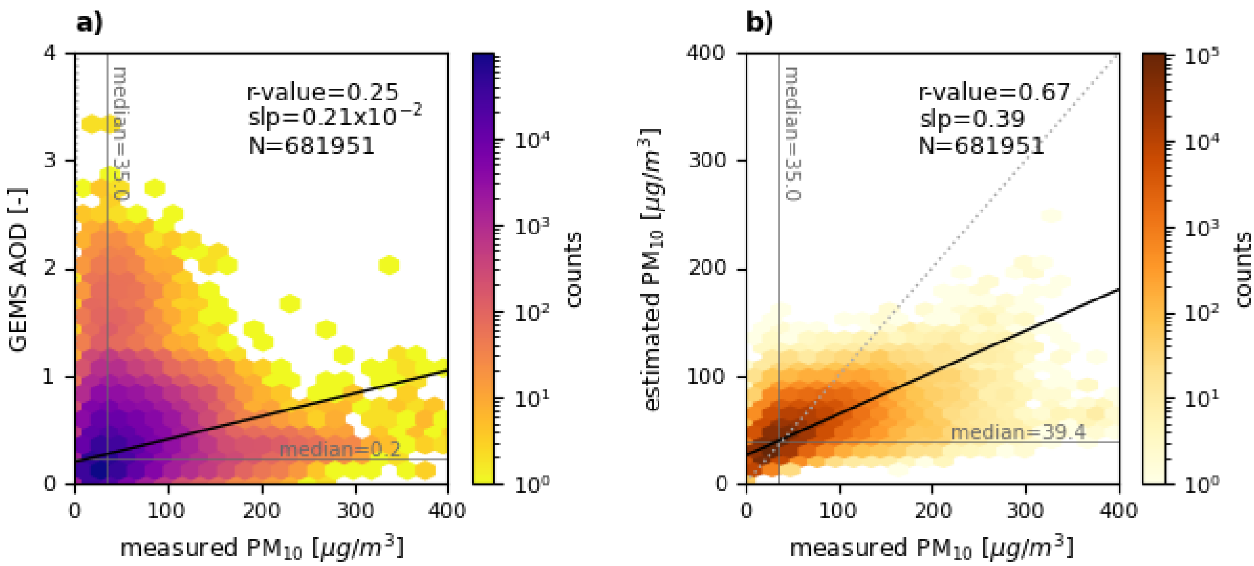

Figure 2. Performance of RF models in estimating ground-level PM10 concentrations. (a) Density scatter plot between the measured PM10 and GEMS AOD values across all stations. (b) Density scatter plot between the measured PM10 values and the PM10 values estimated using RF models. The vertical and horizontal lines represent the corresponding median values. The thick solid line is the regression line, and the dotted diagonal line is the one-to-one.

https://doi.org/10.5194/amt-2024-142
Preprint. Discussion started: 26 August 2024

Atmospheric Measurement Techniques
Discussions

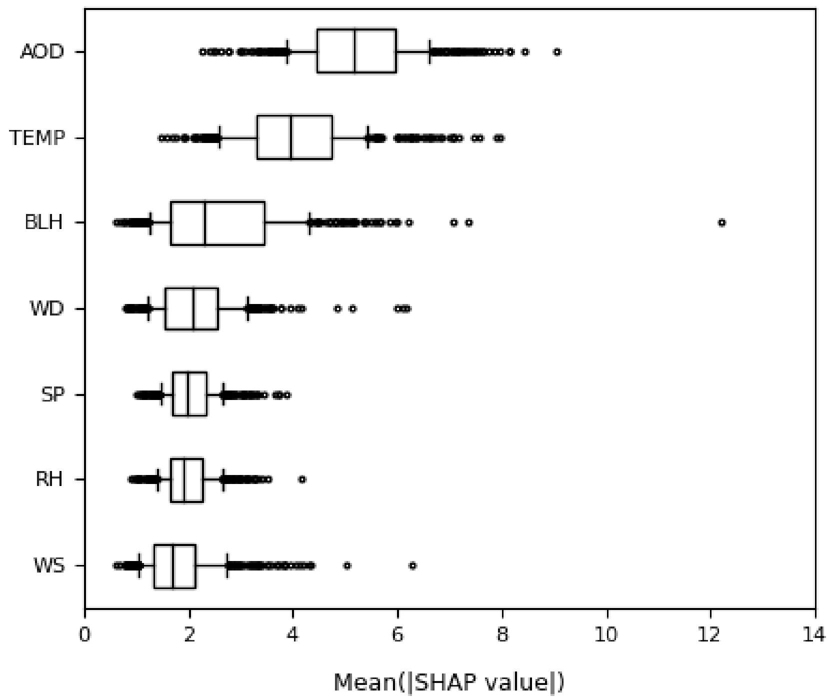

Figure 3. Input importance of RF models. SHAP values are computed to examine the contribution of each input feature to individual predictions. In this box plot, the relative importance of the input variables is shown by ranking the averaged absolute SHAP values. The box represents the interquartile range, the vertical centre line is the median, and the whiskers represent the 10th and 90th percentiles, with outliers shown as dots.

https://doi.org/10.5194/amt-2024-142
Preprint. Discussion started: 26 August 2024

Atmospheric Measurement Techniques Discussions

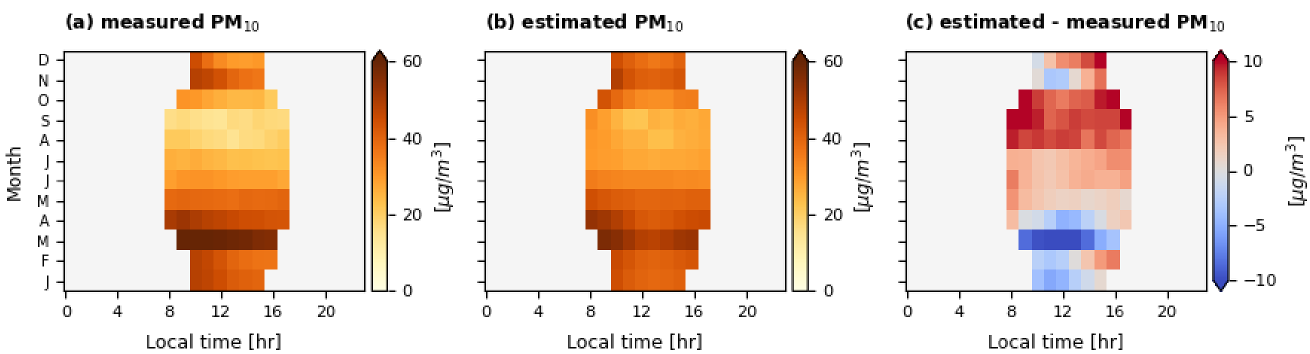

Figure 4. Time-month diagram of PM10 measurements and estimates. The mean hourly (a) measured and (b) estimated PM10 concentrations for each month averaged across all the stations. (c) represents differences between the PM10 measurements and estimates.

https://doi.org/10.5194/amt-2024-142
Preprint. Discussion started: 26 August 2024

Atmospheric Measurement Techniques
Discussions

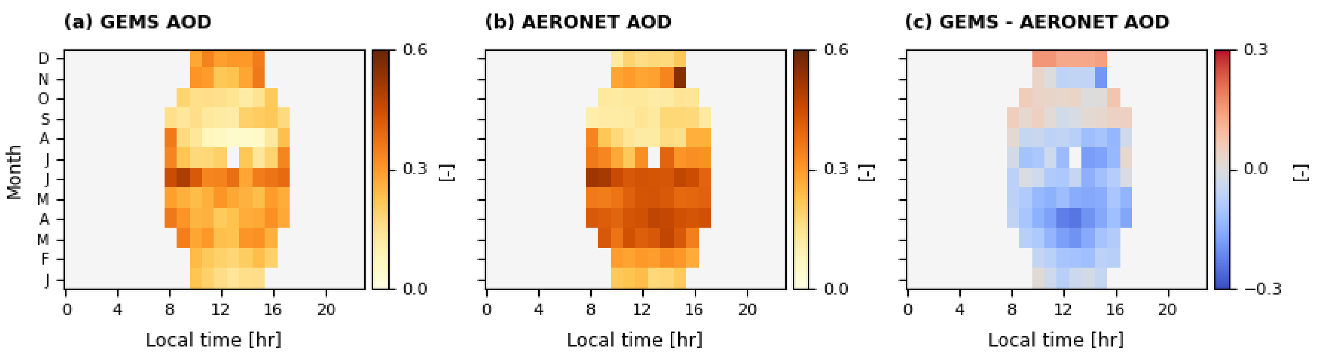

Figure 5. Time-month diagram of GEMS AOD and AERONET AOD. The mean hourly (a) GEMS AOD and (b) AERONET AOD for each month averaged across all the AERONET sites. (c) represents differences between the GEMS and AERONET AOD data. Locations of the AERONET sites can be found in Fig. S7.

https://doi.org/10.5194/amt-2024-142
Preprint. Discussion started: 26 August 2024

Atmospheric Measurement Techniques
Discussions

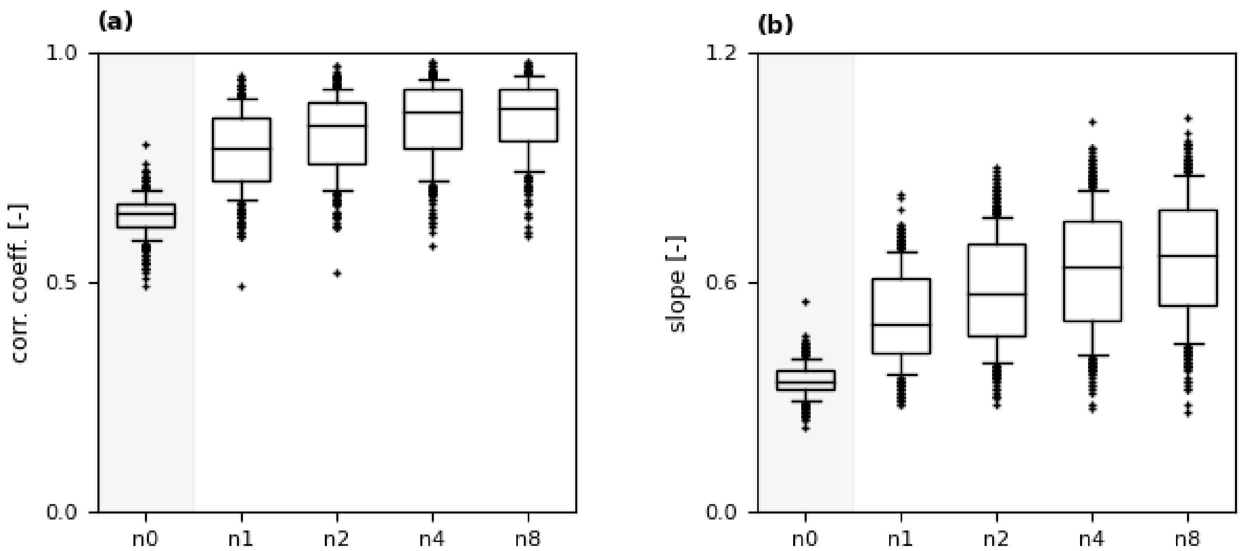

Figure 6. Potential of larger training data in improving the PM10 estimation. (a) Correlation and (b) slope of the linear regression between the measured and estimated PM10 concentrations at each station. Data from the n closest neighbouring sites are additionally used to train the RF models, and the model performance is then re-evaluated through the five-fold cross-validation; the model without neighbouring sites (i.e. $n = 0$) is the model used in the main analysis.